MDPI

Some Recent Advances in Germanium Recovery from Various Resources

Francisco Jose Alguacil *[ID] and Jose Ignacio Robla *[ID]

Centro Nacional de Investigaciones Metalurgicas (CSIC), Avda. Gregorio del Amo 8, 28040 Madrid, Spain
* Correspondence: fjalgua@cenim.csic.es (F.J.A.); jrobla@cenim.csic.es (J.I.R.)

Abstract: Though nowadays germanium does not reach the range of popularity of other metals, i.e., rare earth elements, its utility in target industries makes it a strategic metal. Though germanium can be found in a series of raw materials, the principal source for its recovery is from secondary wastes of the zinc industry; also, the recyclability of germanium-bearing waste materials is becoming of interest. In this recovery and due to the size of the target materials, because the diffusion and reaction are to be considered, hydrometallurgy performs a key role in achieving this goal. The present work reviews the most recent applications (2023 and 2024 years) of hydrometallurgical operations on the recovery of germanium from different solid and liquid sources.

Keywords: germanium; recovery; leaching; liquid-liquid extraction; adsorption; ion exchange

1. Introduction

Germanium is an element that, like many others, has undergone variations over the years in its strategic value, i.e., in 2011, the total germanium production (140 t) exceeded the worldwide necessities (110 t) but in recent times, the situation has dramatically changed, with the total production (142 t in 2021) being below worldwide germanium demands (173 t in 2019 and growing) [1,2]. This element, which has no significant biological role, is being used in optical fibers, infrared optics, polymer catalysts, electronics, solar, etc. Besides the recovery of this element from secondary sources, germanium can be found in sulfide deposits (USA, Mexico, Argentina, Canada, Russia) and oxidization zones in Ge-bearing sulfide deposits (USA). As it has been recently described in the literature [3], there are three large coal deposits containing germanium: the Spetsugli deposit in the Russian Far East, the Wulantuga deposit of Inner Mongolia (Northern China), and the Lincang deposit in the Yunnan Province (Southwestern China). Another important germanium occurrence is in bornite materials [4], such as the carbonate-hosted bornite Cu-Zn-Co(-Ge) deposit located in the Cosmos Hills (Western Alaska, USA). Other Ge-bearing carbonate-hosted base metal deposits are located in Africa, such as the Tsumeb (Namibia), Kipushi (DRC), Khusib Springs (Namibia), Kombat (Namibia), and Kabwe (Zambia) deposits.

Another potential germanium occurrence is in bitterns (residual brines produced in the solar sea-salt extraction in the Mediterranean Sea region) [5] and, as mentioned above, in subproducts of the zinc industry and in the recycling of electronic wastes [6]. It is estimated that about 30% of germanium production results from the recycling of germanium-bearing materials.

At the time of writing this manuscript (April 2024), the price of this element is $2856.30/kg, which compares well with that of other metals, i.e., Cu ($8.49), La ($625), Nb ($45), Tb ($1460), and Y ($30), but not with, i.e., Au ($70,015) and Os ($14,000) (all prices taken from the Internet during the first week of April 2024).

All of the above is reflected by the fact that germanium is included in the fifth list in 2023 of critical raw materials (CRM) for the European Union [7], though its inclusion in this list can be dated even earlier.

Thus, there is an interest in the recovery of this relatively lesser-known metal from these various sources, being that hydrometallurgical processing is widely used to reach this goal. This manuscript reviewed the most recent advances (years 2023–2024) about the use of these hydrometallurgical operations in the recovery of this valuable and strategic element.
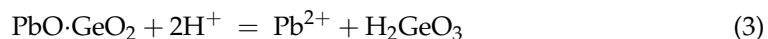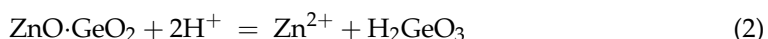
2. Research Methodology

Refs. [8–42] were taken from the Scopus "www.scopus.com" (accessed on March–April 2024) and Web of Science "https://webofscience.clarivate.cn/wos/woscc/basic-search" databases under the terms: germanium recovery, germanium and leaching, germanium and solvent extraction (liquid-liquid extraction), germanium and ion exchange resins, and germanium and adsorption, for the years 2023–2024. It should be mentioned that some journals are currently publishing manuscripts, with dates of November–December 2024, and even 2025.

3. The Hydrometallurgical Operations

3.1. Leaching

Germanium is recovered from a zinc oxide dust subproduct from a Pb-Zn smelter [8]. Since germanium is found to be in different phases (oxide, sulfide, silicate, and solid insoluble), the behavior of these phases in the leaching process is investigated. Under the experimental conditions of a temperature of 85 °C, liquid/solid ratio 7 L/kg, leaching time 3 h, and final pH in the 0.09–0.13 range, a waste electrolyte containing 43.3 g/L Zn, 22.5 g/L Mg, 4.8 g/L Mn, 0.3 g/L Cl, and 160 g/L sulfuric acid has been used to leach the zinc oxide dust containing 1320 g/t germanium. The metal presented in the oxide and sulfide phases dissolve without much difficulty; however, this is not the case of the silicate and solid insoluble phases. The structure of the aluminate phase is destroyed in a leaching operation using 40 g/L HF, whereas dusts containing Fe and Si produced a negative effect in the leaching rate of germanium.

The recovery of germanium from a zinc oxide dust is also investigated in the next Ref. [9]. In this dust, germanium is found as oxidized and germanite species, being that the metal dissolution (Equations (1)–(3)) is dependent on the leaching time; due to this, longer operation times produce the precipitation of $Fe_4Ge_3O_{12}$ species (Equation (4)).

$$GeO_2 + H_2O = H_2GeO_3 \tag{1}$$

$$ZnO \cdot GeO_2 + 2H^+ = Zn^{2+} + H_2GeO_3 \tag{2}$$

$$PbO \cdot GeO_2 + 2H^+ = Pb^{2+} + H_2GeO_3 \tag{3}$$

$$4Fe^{3+} + 3H_2GeO_3 + 3H_2O = Fe_4Ge_3O_{12} + 12H^+ \tag{4}$$

The best experimental conditions to yield the highest germanium recovery rate (84%) are fixed as: liquid/solid ratio of 5, temperature of 85 °C, leachant (sulfuric acid) concentration of 120 g/L, and operation time of 30 min. The addition of sodium sulfite in the leaching process increases the germanium recovery rate until 89%, due to the inhibition of the iron(II) oxidation to iron(III), avoiding the further precipitation of the Fe-Ge mixed oxide.
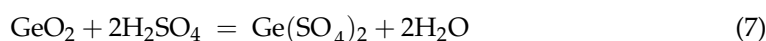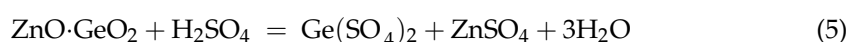
As mentioned in the Introduction section, coal deposits are a source of germanium recovery; thus, in the next reference coal fly ash (CFA), produced in coal-fired power plants, is used as a source material for the recovery of germanium and other metals (vanadium and lithium) [10]. A spent-medium bioleaching process, with *Pseudomonas putida* and *Pseudomonas koreensis*, is used to produce organic acids (Table 1), which dissolves these metals. Previously to this leaching step, the starting material is roasted in the presence of sodium carbonate. Best leaching results (83% germanium recovery) are obtained when *Ps. Putida* is used to produce the organic acids. This recovery rate compares well with the value (58%) obtained when the roasted material is chemically leached with the same organic acids, and this behavior is attributable to other metabolites, such as amino acids and undetermined organic acids, which may be involved in the leaching process.

Table 1. Organic acids produced as a consequence of using *Ps. putida* and *Ps. koreensis*.

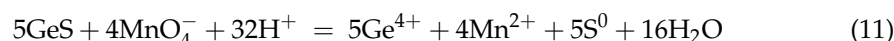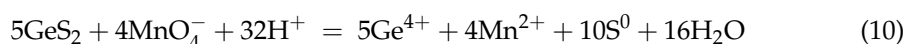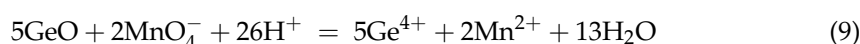| Acid	*Ps. putida*	*Ps. koreensis*
Citric	7.23 mM	6.97 mM
Gluconic	65.76 mM	55.06 mM
Oxalic	11.66 mM	0.78 mM

Adapted from Ref. [10]. mM = millimole.

Using a zinc oxide dust, the recovery of germanium utilizing sulfuric acid and sonication is investigated [11]. The use of ultrasonic (270 W) allows for the recovery of 95% of the initial germanium content (661 g/t) of the starting material, with the other parameters fixed as: 78 °C, 131 g/L of sulfuric acid, 22 min of reaction time, liquid/solid ratio of 7.6, and a 0.71% addition of iron powder. It is concluded that sonication destroyed dust particles, inhibited its agglomeration, and favored the dissolution of germanites and germanium sulfide species. The reactions involved in the dissolution of germanium are:

$$ZnO \cdot GeO_2 + H_2SO_4 \ = \ Ge(SO_4)_2 + ZnSO_4 + 3H_2O \tag{5}$$

$$ZnS \cdot GeO_2 + 2O_2 + 2H_2SO_4 \ = \ Ge(SO_4)_2 + ZnSO_4 + 2H_2O \tag{6}$$

$$GeO_2 + 2H_2SO_4 \ = \ Ge(SO_4)_2 + 2H_2O \tag{7}$$

$$FeGeO_3 + 3H_2SO_4 \ = \ FeSO_4 + H_2GeO_3 \tag{8}$$

The recovery of germanium using zinc powder replacement residue (ZPRR) in a two-stage acid leaching process is investigated [12]. In the first stage, the dissolution uses a solution of 15 g/L sulfuric acid, whereas in the second stage, the material is leached by means of a 150 g/L sulfuric acid solution. The increase in temperature produces an increase in the metal leaching rate; however, at 120 °C, this leaching rate decreases due to the precipitation of germanium in the presence of SiO_2. This precipitation can be avoided by combining temperature, strong magnetic field, and sonication. Within optimal conditions, the rate of germanium leaching reached 97%.

A three-step procedure (leaching-roasting-leaching) of a zinc oxide dust to recover germanium is investigated [13]. Firstly, the dust is leached under sonication and oxidation (potassium permanganate) conditions in order to improve the solubilization of oxidized and sulfide phases:

$$5GeO + 2MnO_4^- + 26H^+ \ = \ 5Ge^{4+} + 2Mn^{2+} + 13H_2O \tag{9}$$

$$5GeS_2 + 4MnO_4^- + 32H^+ \ = \ 5Ge^{4+} + 4Mn^{2+} + 10S^0 + 16H_2O \tag{10}$$

$$5GeS + 4MnO_4^- + 32H^+ \ = \ 5Ge^{4+} + 4Mn^{2+} + 5S^0 + 16H_2O \tag{11}$$

Further, the residue of the previous operation is roasted in the presence of sodium carbonate and magnesium nitrate, which promotes the reaction between the insoluble tetrahedral germanium dioxide and complex forms of germanium-containing compounds:

$$GeO_2 + Na_2CO_3 \ = \ Na_2GeO_3 + CO_2 \tag{12}$$
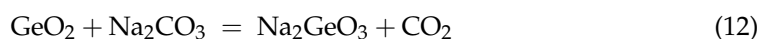
In the third operation, germanium in the roasting slag is recover by conventional leaching. The recovery of this strategic metal increases up to 40% in respect to previous results.

By combination of atmospheric pressure leaching and oxygen pressure leaching methodologies, the dissolution of indium and germanium from a complex matrix formed by oxides, sulfides, germanites, ferrites, and silicates is investigated [14]. The results show that both indium and germanium solubilize from oxide and germanite matrices under atmospheric pressure leaching conditions (80 °C, 3 h, 180 g/L sulfuric acid). Refractory compounds can be leached under conditions of pressure leaching (120 °C, 3 h, 0.25 MPa, 180 g/L sulfuric acid). Using these two operations, the leaching rate reached more than

95% each for indium, germanium, copper, and zinc. Apparently, authors do not include information about the separation of the different metals from the leaching solution.

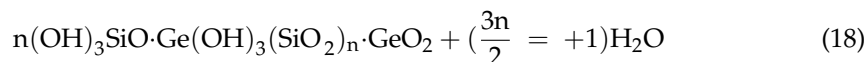The acidic leaching process was used in the dissolution of germanium from low germanium bearing silica residue (GRS) with high silicon content [15]. The responsible reactions for germanium leaching are:

$$Zn_2GeO_4 + 2H_2SO_4 = 2ZnSO_4 + Ge(OH)_4 \tag{13}$$

$$Ge(OH)_4 = H_2GeO_3 + H_2O \tag{14}$$
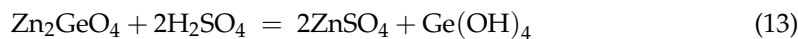
In comparison with the non-pressure procedure, the leaching of the germanium-bearing material at a high pressure yielded a higher germanium leaching rate, i.e., at 240 °C, this rate reached 74%, a value 3.5 times greater than that obtained from the conventional acid leaching process. Moreover, the increase in temperature from 120 °C to 240 °C increased the germanium leaching rate, since at the higher temperature the depolymerization and polycondensation reaction of polysilicic acid is increased, resulting in the conversion of silicon into dense oligomeric silica with a low specific surface area:

$$O_{(n-1)}Si_n(OH)_{(2n+2)} + Si(OH)_4 = O_nSi_{(n+1)}(OH)_{(2n+4)} + H_2O \tag{15}$$

$$nSi(OH)_4 = (SiO_2)_n + 2n(H_2O) \tag{16}$$
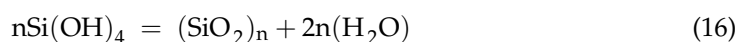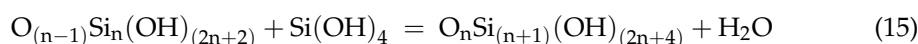
Within this conversion, the encapsulation (adsorption) of germanium on silicon is inhibited, favoring the metal leaching:

$$nSi(OH)_4 + Ge(OH)_4 = n(OH)_3SiO \cdot Ge(OH)_3 + H_2O \tag{17}$$

$$n(OH)_3SiO \cdot Ge(OH)_3(SiO_2)_n \cdot GeO_2 + (\frac{3n}{2} = +1)H_2O \tag{18}$$

Problems in relation to the presence of tannin in zinc electrolysis, neutralization, and the precipitation-leaching procedure was investigated in order to replace Ge precipitated by tannin to enrich Ge [16]. The leaching solution of zinc oxide dust was used as a raw material and industrial zinc oxide dust was used as a neutralizing agent. Under conditions of neutralization-precipitation at 45 °C, 2 h, pH 5.0–5.2 (first stage) and 45 °C, 1.5 h, oxygen dosage 60 L/h, pH 5.0–5.2 (second stage), the precipitation rates were 99% (Ge), 27% (Fe), 99% (As), and 95% (Si). The neutralizing sediment contains 1.1% Ge in the first stage and a germanium concentration in the second stage solution of nearly 2 mg/L. The leaching residue after oxidative pressure leaching is leached under atmospheric pressure, increasing the leaching rate of germanium increases to 96%. Though the procedure resulted in the simultaneous germanium enrichment and impurity removal, no data is included in the work about how to separate germanium from undesirable impurities.

The leaching of zinc and germanium from a zinc oxide dust by a combination of ultrasonic and hydrazine sulfate was investigated [17]. It was established that the best results necessitated the reduction of both Ge(IV) and Fe(III) to Ge(II) and Fe(II), respectively. The final mixed controlled model is determined to control the whole leaching reaction. Under the best conditions of initial acidity of 140 g/L, liquid/solid ratio 7 L/kg, dosage of the reducing agent of 1/3 of the molar mass of Fe in zinc oxide dust, ultrasonic intensity of 300 W, 1 h, 60 °C, the leaching rates are 97% (Zn) and 95% (Ge). In comparison with the results under conventional leaching, the leaching rates increased by 6% (Zn) and 11% (Ge). Again, no data about the separation of these metals are included in the work. Moreover, the potential toxicity of hydrazine and related compounds [18], i.e., hydrazine sulfate, could be an odd point for the future development and potential scaling up of the proposed procedure.

To resolve some problems arising in the treatment of germanium-zinc leaching residue, the next investigation used a two-stage countercurrent pressurized acid leaching technique [19], which consisted of (i) iron-controlled low-acid pressure leaching and (ii) deep

high-acid pressure leaching. Experimental data indicated that the increase of in temperature, reaction time, and oxygen partial pressure enhanced the dissociation of zinc-loaded and germanium ferrite ($MeFe_2O_4$) complex phases and facilitated the occurrence of Fe(III) hydrolysis and precipitation. Under the optimized conditions of 150 °C, initial acidity of 100 g/L, reaction time of 3 h, and oxygen partial pressure of 0.4 MPa, the leaching rates of zinc and germanium are nearly 92% and 61%, respectively. No data about the separation of the metals are included in the work.

The results derived from the investigations about germanium recovery from these different germanium-bearing materials are summarized in Table 2.

Table 2. Germanium recoveries from several secondary materials.

Material	Ge Content, g/t	Leachant	% Ge Recovery	Ref.
ZOD	1320	Waste electrolyte	80	[8]
ZOD	418	Sulfuric acid	84	[9]
CFA	250	Organic acids	83	[10]
ZOD	661	Sulfuric acid [a]	95	[11]
ZPRR	1500	Sulfuric acid [b]	97	[12]
ZOD	2000	Sulfuric acid [c]	95	[13]
GRS	2.8	Sulfuric acid [d]	74	[15]
ZOD	510	Sulfuric acid [e]	95	[17]

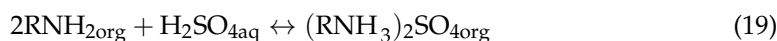ZOD: zinc oxide dust. CFA: coal fly ash. ZPRR: zinc powder replacement residue. GRS: germanium silica residue. [a] Acid and sonication. [b] Two steps. [c] Three steps: acidic leaching, roasting, and acidic leaching. [d] Acid plus temperature and high pressure. [e] Acid and reduction.

Table 2 indicates that these recent investigations used secondary materials as the initial source for germanium recovery and that, in all the acceptable cases, rate recoveries with most of the proposed different leaching systems are obtained. However, no one reference included in this table indicates what to do with the germanium-bearing solution or how this strategic metal can be recovered from the different leachates.

3.2. Liquid-Liquid Extraction

Ionic liquids are a group of chemicals that, due to their properties, are broadly considered as green solvents. This Ref. [20] reviews the use, on germanium extraction, of one specific type of these extractants based on the phosphonium ion (R_4P^+), where R represented various carbon-based chains. The counter anion for this phosphonium moiety can be of inorganic or organic nature. The review concluded that phosphonium-based ionic liquids extracted germanium via an anion exchange mechanism and that, due to its specific properties: good selectivity, high thermal stability, and low volatility, this type of extractant presented promising characteristics for its use in the recovery of this valuable metal.

Germanium is recovered from a solution (49 mg/L Ge, 48 g/L Zn, 0.19 g/L Fe, 1.07 g/L As, and 0.33 g/L Cd) after the treatment of a secondary zinc oxide with a 75 g/L sulfuric acid solution [21]. In this investigation, the organic phase contains the primary amine N1923 (RNH_2) and tributyl phosphate (TBP) as phase modifier, dissolved in sulfonated kerosene; to this organic phase, different concentrations of hydroxycitric acid (HCA, 1,2-Dihydroxypropane-1,2,3-tricarboxylic acid) are added. With the metal equilibrium extraction reached after six minutes, germanium is extracted (80–99%) preferably to the other metals present in the solution in the equilibrium pH range of 0.1–2.5. As mentioned above, TBP is needed in order to avoid third phase (or secondary organic phase) formation (Figure 1). The best germanium extraction results are reached under the conditions: equilibrium pH of 1, 20% *v/v* amine, 5% *v/v* TBP, and a molar ratio of CHA/Ge of 5. The reactions involved in the extraction of germanium are:
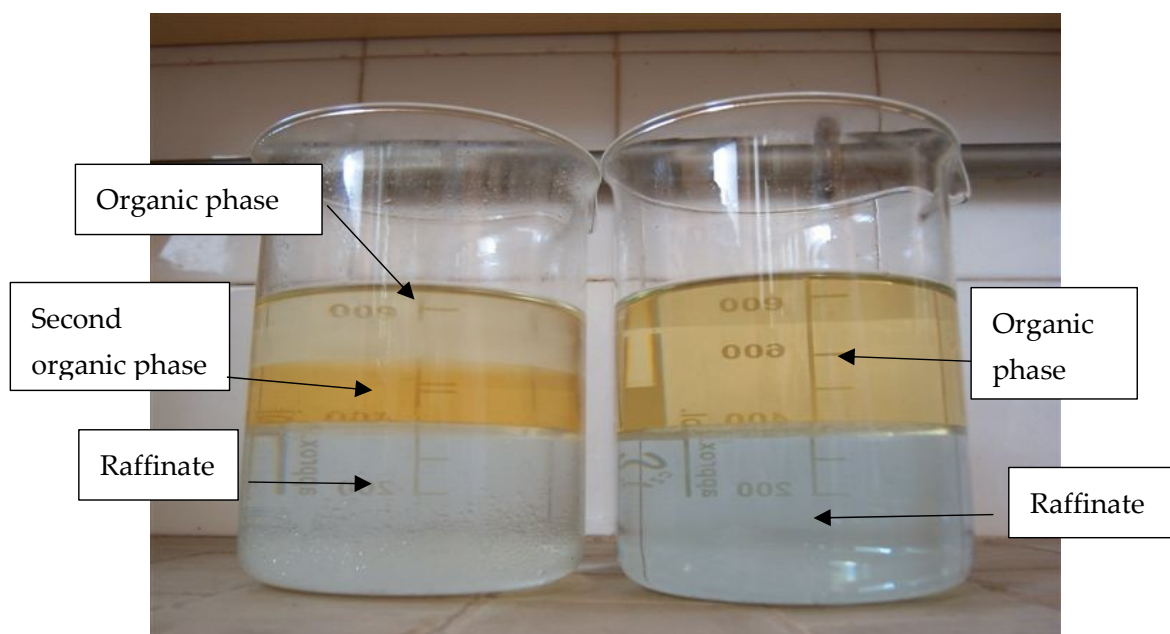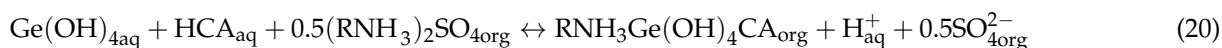
$$2RNH_{2org} + H_2SO_{4aq} \leftrightarrow (RNH_3)_2SO_{4org} \tag{19}$$

$$Ge(OH)_{4aq} + HCA_{aq} + 0.5(RNH_3)_2SO_{4org} \leftrightarrow RNH_3Ge(OH)_4CA_{org} + H^+_{aq} + 0.5SO_{4org}^{2-} \tag{20}$$

Figure 1. Undesirable third phase formation (two organic phases) (left) in liquid-liquid extraction vs. ordinary two-phase systems (right). (Picture by F.J.Alguacil).

In the above equations, the subscripts aq and org refer to the species found in the aqueous and organic phases, respectively. The system also investigates simulated solutions derived from the treatment of copper cake, coal fly ash, and biomass. A 0.5 M NaOH solution is an effective strippantr for germanium (and arsenic). No data is provided in the reference as to how these two elements can be separate from the stripping solution. Moreover, Equations (19) and (20), as written in the published reference, are badly unresolved, since in Equation (19) the species formed in the organic phase, being an amine salt or a pseudo-protic ionic liquid, must be formulated as $(RNH_3^+)_2SO_4^{2-}$. With respect to Equation (20), as well as having the same problem with the amine compound, in the CA^- species, the right side of the equation is clearly unbalanced in the number of protons on each side of the equilibrium.

Using simulated sulfuric acid solutions, the extraction of germanium using the tertiary amine N235 (R_3N, $R = C_8H_{17}$) in the bisulfate cycle dissolved in sulfonated kerosene is investigated [22]. The addition to the organic phase of trioctyl phosphate (TOP) and L(+)-tartaric acid (H_2L) is also considered. TOP avoids the formation of a third phase after equilibration of the phases and participates in the formation of extraction complexes through hydrogen bonds in the form of Ge–OH$\cdots$O[dbnd]P but does not co-extract germanium with the amine. In fact, it is described that the metals are extracted into the organic phase via an anion exchange mechanism, with formation in the organic phase of $Ge(OH)(HL)_2L \cdot HNR_3$ and $Ge(OH)(HL)L_2 \cdot (HNR_3)_2$ species. This work does not provide data about the stripping operation; thus, the usefulness of its utility must be put into quarantine. Also, it is strange that the authors use as extractant a tertiary amine in the bisulfate cycle ($R_3NH^+HSO_4^-$) when the known rule is that tertiary amines are most effective (and broadly used) as extractants of metals in the chloride cycle ($R_3NH^+Cl^-$).

Liquid-liquid extraction of germanium from a leaching solution of 0.53 g/L Ge, 93 g/L Zn, 7.6 g/L Fe, 1.5 g/L Cu, 0.64 g/L Cl, 0.66 g/L F, and 67 g/L sulfuric acid, with organic phases containing hydroxamic acid (YW100), di(2-ethylhexyl) phosphoric acid (D2EHPA),

and the tertiary amine (N235) is investigated [23]. Kerosene is used as a diluent of the organic phase. The extraction equilibrium is represented as:

$$Ge_{aq}^{4+} + 3(HR)_{org} + (H_2A_2)_{org} \leftrightarrow GeR_3 \cdot HA_{2org} + 4H_{aq}^+ \tag{21}$$

In the above equilibrium, HR represented the YW100 molecule, whereas H_2A_2 represented the dimeric form of D2EHPA. Though the authors claim that the formation of a third phase is avoided with the use of the amine, in the opinion of these reviewers, and after looking at Figure 2 in the published Ref. [23], this third phase is not avoided completely and, thus, the data presented here are useless and the manuscript should never have been published. Note also the bad use of non-existent Ge^{4+} species in Equation (21).

This reference investigates the extraction of germanium from wet zinc refining solutions using the mixture of the amine N325 and the phosphorus ester tributylphosphate (TBP) [24]. This last chemical is utilized as a modifier to prevent the formation of a third phase. The extraction mechanism responded to an anion exchange process in which $(Ge(C_4H_4O_6)_3{}^{2-})$ species formed part of the extracted complex, where $C_4H_4O_6{}^{2-}$ represented the tartrate anion. The system is selective with respect to the presence of As^{3+}, Fe^{2+}, and Zn^{2+} in the feed solution. Germanium can be stripped from the organic solution by the use of 2.5 M NaOH solutions. Note the major mistake done by the authors when As(III) is considered a cation, since this element is never found as a cation in aqueous solutions.

This manuscript, very similar to the previous reference, investigates the extraction of germanium(IV) by the same system amine N235 and TBP but using different metal-coordinated complexes [25]. The coordination abilities follow the sequence: tartaric acid > oxalic acid > citric acid > maleic acid > salicylic acid. Here again the authors committed a major fault by considering germanium(IV) as the cation Ge^{4+}.

The next Ref. [26] investigates the indium-germanium separation from a leaching solution containing, among others, 2.45 g/L In, 0.11 g/L Ge, and 37 g/L sulfuric acid. The procedure consisted of two steps. In the first step, indium is separate from germanium by liquid-liquid extraction with an organic phase of 15% *v/v* DEHPA in kerosene; in the second step the germanium-bearing raffinate from this liquid-liquid extraction operation is neutralized with ZnO dust until pH values are in the 3.5–4.0 range, and is then mixed with tannin:

$$Ge^{4+} + H_2T \rightarrow GeT^{2+} + 2H^+ \tag{22}$$
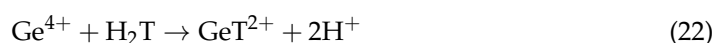
By this procedure, germanium is quantitatively (99%) precipitated as a tannin-germanium complex. This solid is calcined at 500 °C during 3 h to yield a germanium concentrate.

3.3. Ion Exchange Resins

In this Ref. [27], the anion exchange resin D201×7 (strongly basic styrene-based anion exchange resin with quaternary ammonium group (R_3R'-N^+ being R = CH_3 and R' = Cl) and chloride as counter-anion) has been used to separate germanium from a sulfuric solution, using tartaric acid as a complexing agent. In the sulfuric acid system, $Ge(OH)_4$ was converted to an anionic complex $[GeO_2(OH)_2C_4H_4O_4]^{2-}$ at a 1:1 tartaric acid-to-metal molar ratio, and thus, the resin uptakes this anionic complex. The anionic exchange process fits the pseudo-second-order kinetic and Langmuir isotherm models. Maximum metal loading onto the resin is estimated as 214 mg/g. At pH 2, and using single metal solutions, the rate of germanium loaded onto the resin is better than that of iron(III), but using mixed Ge(IV)-Fe(III) solutions, this situation is reversed and iron(III) is loaded preferably to germanium(IV). Elution of germanium from loaded resin is best accomplished with the use of 1 M NaOH solutions. Moreover, selective germanium uptake and purification are enhanced in column operations. The results show that with an enrichment factor of 74.7, the concentration of germanium in the eluate reached 36.6 g/L.
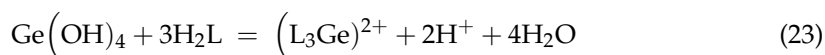
3.4. Adsorption

This reference investigated the mechanism of germanium adsorption onto lead sulfate and uses ultrasonication to inhibit this adsorption [28]. Results concluded that the adsorption process fits the pseudo-second-order kinetic and Langmuir isotherm models. Germanium adsorption onto lead sulfate consists of three steps: fast, slow, and equilibrium. The adsorption at 25–55 °C is a spontaneous, endothermic, and entropy increasing process, while at 55–85 °C it is a spontaneous, exothermic, and entropy decreasing process. Increasing of the ultrasonic power in the 0–22.5 W increases germanium uptake onto lead sulfate, though a further increase of the ultrasonication up to 70 W decreases the metal uptake, and thus, the adsorption of germanium onto lead sulfate is inhibited (Table 3).

Table 3. Equilibrium germanium uptakes vs. ultrasonic power.

Ultrasonic Power, W	$[Ge]_{eq}$, mg/g
0	$10 < x < 10.5$
15	$13.5 < x < 14$
22.5	$14 < x < 14,5$
30	$11.5 < x < 12$
45	$9 < x < 9.5$
75	7.5

Initial germanium concentration: 3.4 g/L. Lead dosage: 3 g. Temperature: 85 °C. Adapted from Ref. [28].

In the next investigation [29], a microwave-based synthesis method is used for functionalized polystyrenic beads with catechol (A-Cat), nitro-catechol (A-Cat-N), and pyrogallol (A-Py). These adsorbents have been used in the selective removal of germanium from dilute acidic solutions under various experimental conditions. The metal adsorption fits the Langmuir isotherm with uptakes at pH 3 of 29.76 mg/g, 39.14 mg/g, and 37.13 mg/g, for A-Cat, A-Cat-N, and A-Py, respectively. The adsorption mechanism responds to surface complexation of germanium with the ligand (i.e., catechol):

$$Ge\left(OH\right)_4 + 3H_2L = \left(L_3Ge\right)^{2+} + 2H^+ + 4H_2O \tag{23}$$

The adsorbents were highly selective for germanium against other elements at pH 1–3, showing no adsorption for many competitive ions: (Be(II), Mg(II), Al(III), Sc(III), Mn(II), Fe(III), Cu(II), Zn(II), Ga(III), As(V), Cd(II), La(III), Yb(III), Pb(II), Th(IV), and U(VI)) at pH 1–2. A-Cat was more selective than A-Cat-N and A-Py. The adsorbents fit the pseudo-second-order kinetic equation. Using A-CAT desorption is best performed with 2 M sulfuric acid solutions.

Catechol-functionalized chitosan (C-Cat) has been synthesized and used to recover germanium from dilute acidic solutions [30]. With maximum metal uptake in the 4–11 pH range, the adsorption fits the Langmuir isotherm and pseudo-second-order kinetic models. Maximum loading capacity reached 22.7 mg/g, which compares badly with the value of 79.7 mg/g resulting from the use of Purolite S108 (N-methylglucamine-based commercial adsorbent), though C-Cat presented a high selectivity for germanium against the presence of other competing ions in the solution. Experimental results show that germanium is adsorbed preferably to Al(III), Cu(II), Zn(II), and Pb(II) (no adsorption of these), with limited adsorption of Fe(III), Ga(III), and As(V). The best desorption results are obtained with the use of 1 M HCl (72%) after 24 h, whereas, in the case of 1 M sulfuric acid, the rate is 65% within the same reaction time. There is a decrease in germanium uptake capacity with consecutive adsorption-desorption cycles, i.e., 20 mg/g in the first cycle and 12 mg/g in the third cycle.

An adsorbent for recovery of germanium is prepared by grafting D-anhydrous glucose onto UiO-66-NH$_2$ (a zirconium-based adsorbent [31]), resulting in a DG-UiO-66 adsorbent [32]. Under the optimum experimental conditions of 25 °C and pH 10, the grafted adsorbent presents a removal rate of 90%, which compares well with that of the pris-

tine adsorbent (80%). The maximum adsorption loading onto the adsorbent is almost 217 mg/g. Similarly to previous references, the adsorption of Ge(IV) fits the pseudo-secondary kinetic and Langmuir isotherm models, with the adsorption mechanism described by the intraparticle diffusion model. The thermodynamic results show that the higher the temperature (25–45 °C range), the stronger the adsorption capacity of Ge(IV), and the reaction is spontaneous. The presence of anions in the feed solution decreases the rate of germanium adsorption (Table 4). Desorption is carried out with a solution of 10% thiourea and 1% sulfuric acid.

Table 4. Germanium adsorption in the presence of anions.

Anion	Concentration	% Ge Adsorption
Sulfate Chloride	0.1 M	80
	0.5 M	77
	1 M	70
	0.1 M	87
	0.5 M	84
	1 M	82

Adapted from Ref. [32].

A metal-organic framework adsorbent (Ma-Zr-MOF) is synthesized using mucic acid and used to recover germanium from aqueous solutions [33]. The maximum adsorption capacity of germanium by Ma-Zr-MOF is 82 mg/g at 22 °C and pH 6, and again, the adsorption of germanium onto Ma-Zr-MOF responded to the pseudo-second-order kinetic and Langmuir isotherm models. Thermodynamic calculations yield that the adsorption process is endothermic and spontaneous, with an increase in the adsorption capacity with the increase in temperature in the 25–45 °C range. Experimental results concluded that the ortho-hydroxyl group plays a key role in the removal of germanium from the solution and that the adsorption mechanism included chelation and ion exchange processes. Similarly to the previous reference, the adsorption of germanium decreases in the presence of different anions (chloride, sulfate, phosphate, silicate, or carbonate), though, in this case, this interference occurs at anion concentrations as low as 0.1 mM. Germanium is adsorbed preferably to Mn(II), As(III), Zn(II), and Si(IV). Alkaline (NaOH) solutions are not useful to desorb germanium from the loaded adsorbent; compared to the above, the use of nitric acid allows the recovery of germanium from the adsorbent, but there is a continuous decrease in the adsorption capacity with continuous use, i.e., 89% in the first cycle vs. 66% in the fifth cycle.

Poly-dopamine (PDA)-coated magnetic nano-Fe_3O_4 particle composites (Fe_3O_4@PDA) are prepared by a dopamine self-assembly method [34]. Further Fe_3O_4@PDA-PEI composite materials are synthesized through a poly-ethylenimine (PEI) modification reaction. This Fe_3O4@PDA-PEI is used to adsorb germanium at various pH values, with pH 6 being the most adequate for the efficient removal of the metal, as this removal is well-fitted to the pseudo-second kinetic model. Compared to the above adsorbents, germanium uptake on this material fits the Sips model; thus, the adsorption is between single layer and multilayer, and chemisorption plays a role. It is also concluded that complexation coordination is the dominant mechanism of adsorption, with the phenolic hydroxyl and amino groups on the surface of the material playing a determinant role in germanium adsorption.

This reference described the performance of a tartaric acid functionalized chitosan (TA-CS) material as an adsorbent for Ge from a zinc residue leachate [35]. The introduction of tartaric acid onto chitosan results in abundant protonable hydroxyl and carboxyl groups, which provide the material with a buffering capacity under acidic conditions. Adsorption kinetics and isotherms showed an adsorption capacity of 57.28 mg/g for Ge(IV). In binary systems, Ge(IV) is preferentially adsorbed over Zn(II), a major coexisting ion, with a separation factor of 3.22. The immobilization of germanium on tartaric acid is the result of a combination of electrostatic adsorption, complexation, hydrogen bonding,

and ion exchange. Again, the presence of anions (up to 10 mM) in the solution decreases the rate of germanium removal, as this effect is more notorious in the case of SiO_3^{2-} than in the case of SO_4^{2-}, phosphate, and carbonate, while the presence of chloride only slightly influences the removal of the metal from the solution. The usefulness of the adsorbent is also proved in the recovery of germanium from a leaching solution (10.2 g/L Zn, 8.3 g8L Cu, 1.8 g8L Fe(III), 0.24 g/L Ge at an initial pH of 0.17) coming from the treatment of a sampled native zinc residue. With a dosage of 15 g/L TA-CS, the rate of germanium adsorption reached 80%. Desorption is investigated using 0.5 M nitric acid or 0.5 M NaOH solutions, giving the acidic medium the best desorption results, though, when using both types of solutions, there is a decrease in the adsorption capacity after continuous cycles of adsorption-desorption.

Three chitosan-based adsorbents are designed by grafting chitosan with p-hydroxybenzoic acid (HBA-CS), 3,4-dihydroxybenzoic acid (DBA-CS), and 3,4,5-trihydroxybenzoic acid (TBA-CS) and are used on the germanium recovery from solutions [36]. Metal recovery performance is correlated with the arrangement of the active adsorption sites, following the order TBA-CS > DBA-CS > HBA-CS, being that this order is attributable to the steric effect of TBA-CS, which is more ideal than that of the other materials due to the presence of more o-phenolic hydroxyl groups, which enhances its affinity toward germanium. The adsorption behavior of DBA-CS and TBA-CS fit the pseudo-second-order kinetic and Langmuir isotherm models, indicating that it is a single layer and chemisorption process. As in previous cases, the presence of anions (10 mM) decreases the performance of the adsorbent in the order: silicate > phosphate > carbonate > sulfate> fluoride > chloride. At a 1:1 germanium:iron(III) ratio, iron(III) is adsorbed preferably to germanium; however, as the ratio decreases in the 1:2, 1:5, and 1:10 ratios, the rate of germanium adsorption is greater than that of iron(III). Copper and zinc are worse adsorbed than germanium at every germanium:metal ratio (from 1:1 to 1:10). Nitric acid medium is useful to desorb germanium, but at the cost of a sharp reduction of the adsorption efficiency: nearly 60% in the first cycle, to less than 40% in the fifth cycle. Against the title indicates, the investigation is not performed on a zinc residue leachate but on a synthetic solution.

The removal of trace elements (TEs: B, Co, Ga, and Ge) from solar saltworks brines using commercial N-methylglucamine chelating sorbents (S108, CRB03, CRB05) is investigated [37]. The three sorbents revealed a good efficiency in the removal of the four elements. Both B and Ge exhibited the fastest sorption kinetics, reaching equilibrium (>90%) in less than an hour, except for S108, which required 2 h. Elution of the adsorbed metals can be performed by the use of 1 M HCl solutions. No data are included in the manuscript about the separation of the metals from the eluate.

The chelating compound DIAION CRBO2 anionite containing hydroxyl and amine groups had been investigated in the removal of Ge(IV) and Cu(II) from chloride solutions [38]. It is demonstrated that the hydroxyl and amino groups of anionite interacted with germanite and copper(II) ions, forming the corresponding metal-anionite complexes. Germanium(IV) is removed from the solution by the adsorption of germanite acid H_2GeO_3 molecular, as well as meta-germanite $HGeO_3^-$ and germanite GeO_3^{2-} anions. Whereas copper can be desorbed with 2.5% HCl solutions, germanium is desorbed with 2.5% NaOH solutions.

The organic acid-functionalized TiO_2 nanoparticles were synthesized by modifying TiO_2 nanoparticles with organic acids containing different numbers of hydroxyl groups, the content of these groups influenced the Ge(IV) adsorption capacity [39]. The material containing tartaric acid (dihydroxysuccinic acid) TiO_2 (TA-TiO_2-OH), having more hydroxyl functional groups (up to nearly 4.48 mmol/g), presented the highest metal adsorption capacity (near 122 mg/g) at pH 3. Desorption can be done by the use of 1 M HCl solutions, though a decrease in adsorption efficiency is observed after continuous use, attributable to the incomplete germanium desorption after each cycle.

In the process of zinc oxide dust neutralization leaching, there is a loss of germanium caused by its adsorption on colloidal $Fe(OH)_3$. It is demonstrated in [40] that the use of ultrasonication reduced the redox potential of the reaction system and inhibited the formation of colloidal $Fe(OH)_3$. Under the conditions of 30 g/L sulfuric acid, a temperature

of 80 °C, ultrasonic power of 500 W, and a pH adjustment time of zinc oxide slurry within 3 min, the experimental data (Table 5) showed that in conventional processing, the loss rates of the elements were higher than under ultrasonic procedure.

Table 5. Element losses (%) at different operational conditions.

Element	Conventional	Ultrasonication
Ge(IV)	25	7.7
Fe(II)	2.2	4.3
Fe(III)	46	14

Adapted from Ref. [40].

Table 6 summarizes the maximum adsorption capacity of some adsorbents used in the recovery of germanium from different solutions.

Table 6. Maximum germanium uptakes using different adsorbents.

Adsorbent	pH	[Ge], mg/g	Reference
A-Cat.N	3	39	[29]
C-Cat	4	22.7	[30]
DG-UiO-66	10	217	[32]
Ma-Zr-MOF	6	82	[33]
TBA-CS	3	28.3	[36]
TA-TiO2-OH	3	122	[39]

It is worth mentioning that all the investigations in relation to the data presented in Table 6 and its respective references have been carried out on synthetic solutions. Thus, in the experimental conditions, see the pH values, in which these adsorbents actuated are far from adequate for the direct treatment of solutions coming from leaching operations (see Table 2 and related references), which generally use acidic media in excess of 100 g/L sulfuric acid.

Also, a disparity in the maximum germanium uptake concentrations using the different adsorbents can be seen. The above joined with the general loss of loading capacity under various adsorption-desorption cycles made it extremely difficult to assess the benefits of using one or another adsorbent.

4. Miscellaneous Operations

In the recovery of germanium from coal, the formation of the GeO_2-SiO_2 solid solution presents difficulties in the recovery of this metal; thus, a procedure involving the enrichment of germanium in lignite by gravity separation and low-temperature sintering is investigated [41]. In this procedure, gravity separation produced a metal concentration factor in lignite of near 2, whereas the treatment of the sinter at 300–500 °C produced residual ash containing 1.8 g Ge/kg, with a concentration factor in the order of 10.6. As a consequence of the above procedure, more than 90% of germanium in lignite can be recovered by chlorinated distillation.

The combustion of lignite to produce electricity generates coal ash wastes containing arsenic, germanium, and tungsten, and the recovery of these elements, was investigated by a procedure involving sequential vacuum distillation [42]. Arsenic volatilizes first at temperatures under 550 °C; further, germanium and tungsten are volatilized as sulfides by the addition of sodium sulfite. The best conditions for this removal are summarized as: 1050 °C, mass ratio of 0.6, pressure of 1 Pa, and 2 h of reaction time. Condensed products are As_2S_3 and GeS, both for coal fly and coal bottom ashes, whereas $WO_x(x < 3)/WS_2$ and WO_3/WS_2 species are present in the above respective ashes.

5. Conclusions

Though there are some raw materials containing germanium, recent investigations have been developed only in the treatment of real or simulated secondary wastes. In these developments, hydrometallurgy plays a key role, offering different alternatives to recycle germanium from zinc wastes, EoL (end-of-life products), and OFs (spent optical fibers), contributing to sustainable resource utilization. Though bio-hydrometallurgical approaches have not been widely developed for these waste materials at present, the development of these bio-procedures is worthy of future attention. Overall, the investigation of sustainable recovery technologies for germanium (and other valuable metals) from, i.e., EoL or zinc oxide dust products is a determinant for ensuring a stable and reliable supply of this element for high-tech applications. Further advancements in the optimization and implementation of these recovery processes will contribute to the efficient and environmentally friendly recycling of these germanium-bearing raw materials and wastes. However, these advancements need to be done in the treatment of real solid materials/wastes, in the processing of germanium-bearing solutions from these treatments, and preferably on a continuous basis; if not, the mismatch between what the scientists proposed and what the industry needs will be insurmountable.

References

1. Reichl, C.; Schatz, M. *World Mining Data 2023*; Federal Ministry Republic Austria Finance: Vienna, Austria, 2023; ISBN 978-3-901074-54-7. Available online: https://www.world-mining-data.info (accessed on 24 April 2024).
2. MinéralInfo. Le Portail Français des Ressources Minérales non Énergétiques. République Française. Available online: https://www.mineralinfo.fr/fr/substance/germanium-ge (accessed on 24 April 2024).
3. Arbuzov, S.I.; Spears, D.A.; Ilenok, S.S.; Yu Chekryzhov, I.; Ivanov, V.P. Modes of occurrence of germanium and tungsten in the Spetsugli germanium ore field, Pavlovka brown coal deposit, Russian Far East. *Ore Geol. Rev.* **2021**, *132*, 103986. [CrossRef]
4. Jones, A. *Germanium Occurrence in the Bornite Deposit, Southwestern Brooks Range, Alaska*; Colorado School of Mines: Golden, CO, USA, 2021; Available online: https://hdl.handle.net/11124/176411 (accessed on 24 April 2024).
5. Randazzo, S.; Vicari, F.; López, J.; Salem, M.; Lo Brutto, R.; Azzouz, S.; Chamam, S.; Cataldo, S.; Muratore, N.; Fernández de Labastida, M.; et al. Unlocking hidden mineral resources: Characterization and potential of bitterns as alternative sources of critical raw materials. *J. Clean. Prod.* **2024**, *436*, 140412. [CrossRef]
6. Zheng, K.; Benedetti, M.F.; van Hullebusch, E.D. Recovery technologies for indium, gallium, and germanium from end-of-life products (electronic waste)—A review. *J. Environ. Manag.* **2023**, *347*, 119043. [CrossRef] [PubMed]
7. Grohol, M.; Veeh, C. *Study on the Critical Raw Materials for the EU 2023*; European Commission: Brussels, Belgium, 2023. [CrossRef]
8. Chen, C.; Zhen, Y.; Li, C.; Wei, C.; Li, M.; Deng, Z.; Li, X. Leaching behavior of germanium presented in different phases from zinc oxide dust under atmospheric acid leaching conditions. *Int. J. Chem. React. Eng.* **2023**, *21*, 1199–1210. [CrossRef]
9. Liang, M.; Di, H.; Song, L.; Yang, K.; Zhang, L. Study on leaching behaviour of germanium and iron in zinc oxide dust from lead zinc smelting. *Can. Metall. Q.* **2023**, *62*, 573–580. [CrossRef]
10. Rezaei, H.; Shafaei, S.Z.; Abdollahi, H.; Ghassa, S.; Boroumand, Z.; Fallah Nosratabad, A. Spent-medium leaching of germanium, vanadium and lithium from coal fly ash with biogenic carboxylic acids and comparison with chemical leaching. *Hydrometallurgy* **2023**, *217*, 106038. [CrossRef]
11. Song, L.; Zeng, Y.; Liang, M.; Di, H.; Liu, J.; Yang, K.; Zhang, L. Process optimization and mechanism of high-efficiency germanium extracting from zinc oxide dust containing germanium enhanced by ultrasound. *Chem. Eng. Process.* **2023**, *191*, 109439. [CrossRef]
12. Liang, Y.; Luo, B.; Zhao, L.; Chen, L.; Ding, B.; Shen, Z.; Zheng, T.; Guo, Y.; Li, Q.; Zhou, B.; et al. Strong magnetic and ultrasonic fields enhanced the leaching of Ga and Ge from zinc powder replacement residue. *Sep. Purif. Technol.* **2024**, *330*, 125572. [CrossRef]
13. Xu, Y.; Xia, H.; Zhang, Q.; Zhang, L. An original strategy and evaluation of a reaction mechanism for recovering valuable metals from zinc oxide dust containing intractable germanide. *J. Hazard. Mater.* **2024**, *468*, 133766. [CrossRef]

14. Tan, Z.; Zhen, Y.; Jin, X.; Du, M.; Li, X.; Wei, C. Study on intensive leaching of indium and germanium from complex materials containing indium and germanium in zinc smelting. *Zhongnan Daxue Xuebao (Ziran Kexue Ban)/J. Cent. South Univ. (Sci. Technol.)* **2023**, *54*, 2552–2562. [CrossRef]

15. Li, Y.; He, X.; Yang, Y.; Chen, J.; Zhang, Z. High pressure acid leaching of low germanium bearing silica residue (GRS): Characterization of leach residue and mechanistic details of germanium leaching. *Hydrometallurgy* **2023**, *216*, 106015. [CrossRef]

16. Wang, Z.; Deng, Z.; Chen, C.; Dai, X.; Wei, C.; Li, X.; Li, M.; Fan, G. Germanium separation and enrichment in zinc oxide leaching solution. *Zhongnan Daxue Xuebao (Ziran Kexue Ban)/J. Cent. South Univ. (Sci. Technol.)* **2023**, *54*, 2992–3003. [CrossRef]

17. Xu, Y.; Xia, H.; Zhang, Q.; Jiang, G.; Zhang, L.; Xin, C.; Cai, W. Ultrasonic enhanced hydrazine sulfate acid leaching of low-grade germanium dust. *Appl. Energy* **2023**, *332*, 120485. [CrossRef]

18. Ivanov, I.; Lee, V.R. Hydrazine Toxicology. Available online: https://www.ncbi.nlm.nih.gov/books/NBK592403 (accessed on 24 April 2024).

19. Zhang, Z.-Y.; Li, C.-X.; Dai, X.-Z.; Liu, Q.; Zhang, M.; Zhang, Y.-Y.; Lu, Z.-Q. Enhanced dissociation and valuable metal leaching behavior of germanium-zinc leaching residue. *Zhongguo Youse Jinshu Xuebao/Chin. J. Nonferrous Met.* **2023**, *33*, 1659–1671. [CrossRef]

20. Dhiman, S.; Agarwal, S.; Gupta, H. Application of phosphonium ionic liquids to separate Ga, Ge and In utilizing solvent extraction: A review. *J. Ion. Liq.* **2024**, *4*, 100080. [CrossRef]

21. Jiang, T.; Wang, P.; Zhang, T.; Zhu, D.; Liu, Z. A novel solvent extraction system to recover germanium from H$_2$SO$_4$ leaching liquor of secondary zinc oxide: Extraction behavior and mechanism. *J. Clean. Prod.* **2023**, *383*, 135399. [CrossRef]

22. Wang, P.; Liu, Z.; Zhang, T.; Liu, Z.; Zhu, D.; Jiang, T. Extraction mechanism of germanium in sulfate solutions using a tertiary amine (N235)-based solvent extraction system. *Sep. Purif. Technol.* **2023**, *311*, 123305. [CrossRef]

23. Tan, Z.; Zhen, Y.; Wei, C.; Jin, X.; Li, X.; Fan, G.; Luo, X.G. Organic phase modification of YW100 extraction system: Extraction of germanium using YW100 + D2EHPA + N235. *Sep. Purif. Technol.* **2024**, *329*, 125175. [CrossRef]

24. Gu, Z.-H.; Li, C.-X.; Li, C.-W.; Liu, Q.; Zhang, Y.-Y.; Zhang, Z.-Y. Extraction mechanism and selective separation behavio-rofgermanium in hydrometallurgical zinc solution. *Zhongguo Youse Jinshu Xuebao/Chin. J. Nonferrous Met.* **2023**, *33*, 3476–3487. [CrossRef]

25. Gu, Z.; Li, C.; Li, C.; Liu, Q.; Wang, Q.; Song, J.; Wang, Y. Coordination separation pattern and extraction mechanism of germanium in zinc leaching solution by wet process. *Zhongguo Youse Jinshu Xuebao/Chin. J. Nonferrous Met.* **2024**, *34*, 279–291. [CrossRef]

26. Tan, Z.; Jin, X.; Zhen, Y.; Wei, C.; Li, X.; Deng, Z.; Li, M. Recovery of indium and germanium from In-Ge residue leaching solution using solvent extraction and tannin precipitation. *Sep. Purif. Technol.* **2023**, *323*, 124416. [CrossRef]

27. He, C.; Qi, M.; Liu, Y.; Liu, Z.; Wei, Y.; Fujita, T.; Wang, G.; Ma, S.; Yang, W.; Gan, J. Highly selective separation of germanium from sulfuric solution using an anion exchange D201×7 resin with tartaric acid. *Hydrometallurgy* **2024**, *224*, 106230. [CrossRef]

28. Liang, M.; Song, L.; Di, H.; Hong, Y.; Dai, J.; Liu, J.; Yang, K.; Zhang, L. Research on the mechanism of lead sulfate adsorption of germanium and ultrasonic inhibition during the leaching process of zinc oxide dust containing germanium. *J. Saudi Chem. Soc.* **2023**, *27*, 101740. [CrossRef]

29. Patel, M.; Karamalidis, A.K. Microwave-assisted synthesis of catechol-based functionalized adsorbents for selective adsorption of critical element germanium. *Chem. Eng. J.* **2023**, *475*, 146367. [CrossRef]

30. Patel, M.; Karamalidis, A.K. Catechol-functionalized chitosan synthesis and selective extraction of germanium (IV) from acidic solutions. *Ind. Eng. Chem. Res.* **2023**, *62*, 2892–2903. [CrossRef]

31. Tang, J.L.; Chen, Y.B.; Wang, S.X.; Zhang, L.B. Engineering of UiO-66-NH 2 selective and reusable adsorbent to enhance the removal of Au(III) from water: Kinetics, isotherm and thermodynamics. *J. Colloid Interface Sci.* **2021**, *601*, 272–282. [CrossRef]

32. Peng, Z.; Wang, S.; Wu, Y.; Liu, X.; Liu, H.; Zhang, D.; Fu, L. Synthesis of novel MOF for adsorption of germanium: Kinetics, isotherm and thermodynamics. *Micropor. Mesopor. Mat.* **2024**, *363*, 112826. [CrossRef]

33. Peng, Z.; Wang, S.; Wu, Y.; Liu, X.; Zhu, M.; Li, P.; Fu, L. Novel Zr-based MOF with Ortho-hydroxyl group selectively traps germanium from aqueous media. *Sep. Purif. Technol.* **2024**, *338*, 126477. [CrossRef]

34. Xiang, H.; Zhao, F.; Li, X.; Min, X. Preparation and characterization of amino-containing magnetic material and its adsorption performance of Ge(IV). *Xiyou Jinshu/Chin. J. Rare Met.* **2023**, *47*, 252–264. [CrossRef]

35. Xiang, H.; Yang, Z.; Min, X.; Liang, Y.; Peng, C.; Liu, X.; Yuan, R.; Wang, Q.; Zhao, F. Enhanced recovery of germanium(IV) from zinc residue leachate by tartaric acid functionalized chitosan: Experiments and DFT calculation. *Hydrometallurgy* **2023**, *221*, 106121. [CrossRef]

36. Xiang, H.; Zhao, F.; Wu, T.; Zhang, X.; Chai, F.; Wang, Q.; Repo, E.; Min, X.; Lin, Z. Unraveling the steric hindrance roles of the phenolic hydroxyl position on the selective Ge(IV) recovery from zinc residue leachate. *Sep. Purif. Technol.* **2023**, *311*, 123338. [CrossRef]

37. Vallès, V.; de Labastida, M.F.; López, J.; Cortina, J.L. Selective recovery of boron, cobalt, gallium and germanium from seawater solar saltworks brines using N-methylglucamine sorbents: Column operation performance. *Sci. Total Environ.* **2024**, *923*, 171438. [CrossRef] [PubMed]

38. Jafarli, M.M.; Abbasov, A.D. Equilibrium conditions, adsorption, adsorption kinetics of the GeO$_2$-Cu(II)-NaCl system on diaion CRBO2 anionite and desorption mode from spent columns. *Chem. Prob.* **2023**, *21*, 64–71. [CrossRef]

39. Yu, H.; Pan, Y.; Zhang, Y.; Gong, L.; Lou, Z.; Shan, W.; Xiong, Y. Surface functional group nanoarchitectonics of TiO$_2$ nanoparticles for enhanced adsorption Ge(IV). *J. Taiwan Inst. Chem. Eng.* **2023**, *143*, 104716. [CrossRef]

40. Song, L.; Liang, M.; Zeng, Y.; Dai, J.; Liu, J.; Yang, K.; Zhang, L. Study on the mechanism of ultrasonic inhibition of germani-um adsorption by Fe(OH)$_3$ in the neutralization leaching section of zinc oxide dust. *Coll. Polym. Sci.* **2023**, *301*, 1185–1196. [CrossRef]
41. Bo, W.; Wu, J.; Miao, Z.; Wan, K. Germanium extraction from lignite using gravity separation combined with low-temperature sintering and chlorinated distillation. *Sep. Purif. Technol.* **2024**, *329*, 125215. [CrossRef]
42. Wang, Z.; Sun, J.; Zhang, L. Separation and recovery of arsenic, germanium and tungsten from toxic coal ash from lignite by sequential vacuum distillation with disulphide. *Environ. Poll.* **2024**, *340*, 122775. [CrossRef]